J. Fluid Mech. (1974), *vol.* 64, *part* 4, *pp.* 817–826
Printed in Great Britain

Stokes flow about a sphere attached to a slender body

By N. J. DE MESTRE† AND D. F. KATZ
Department of Applied Mathematics and Theoretical Physics,
University of Cambridge

(Received 14 January 1974)

Stokes flow is analysed for a combination body, consisting of a sphere attached to a slender body, translating along its axis in an infinite and otherwise undisturbed fluid. The cross-section of the after-body, or tail, is circular; the radius, while not necessarily constant, is small compared with the radius of the spherical head. The tail is represented by a distribution of Stokeslets of strength per unit length $F(z)$, located and directed along its axis. The interactive effect of head–tail attachment is manifested by the presence of image singularities located within the sphere. The image system for a single tail Stokeslet must be such that the no-slip condition is satisfied on the surface of the sphere. It is shown that this system consists of a Stokeslet, a Stokes doublet (stresslet only) and a source doublet located at the image point. The strength $F(z)$ is obtained by applying the no-slip condition to the combination body. The solution follows the lines of traditional slender-body theory, an expansion being performed in ascending powers of the reciprocal of the logarithm of the aspect ratio. The integral force parameters and $F(z)$ are obtained to second order. The interactive effect is assessed, and the results are discussed in the context of a sedimenting micro-organism, such as a spermatozoon. The drag on the combination body is shown to be less by around 10 % than the sum of the drags on an isolated sphere and tail. This drag, for a sperm-shaped body, is divided approximately equally between head and tail.

1. Introduction

An analysis of low-Reynolds-number flow past a combination body consisting of a sphere attached to a slender body is of both fundamental and applied interest. It incorporates slender-body theory into a study of flow about a more generally shaped body, and it provides an improved description of the passive sedimentation of a uniflagellated micro-organism, such as a spermatozoon. Such a study also has some qualitative bearing on resistive-force theories of flagellar locomotion, suggesting how the presence of an attached head affects the local forces per unit length along the tail. In this paper we consider a sphere of radius a attached to a straight slender rod of radius R and length $2l$. The combination body, spherical head forward, translates with velocity U along its axis in an

† Present address: Department of Mathematics, Royal Military College, Duntroon, Australia.

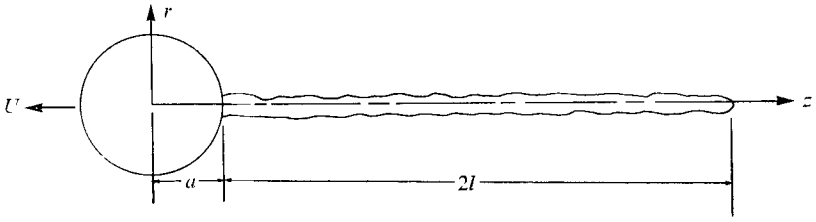

FIGURE 1. The combination body.

otherwise undisturbed fluid of infinite extent. We assume that the Reynolds number of the flow is sufficiently small that the Stokes equations apply; since we are primarily concerned with the forces acting on the body, the need for an outer, Oseen solution does not therefore arise. We also assume $R/2l \ll 1$, i.e. the after-body, or tail is slender, and $R/a \ll 1$. These assumptions are appropriate for the applications mentioned above, and they enable us to incorporate the methods of slender-body theory in the analysis. We shall require here that the cross-section of the tail remain circular, though not necessarily of constant radius. The analysis can, however, be extended to straight slender rods of arbitrary cross-section, using the technique introduced by Batchelor (1970).

2. The image system

Since the tail is slender and the body motion is a simple translation along its axis, the effect of the tail on the fluid may be approximately assessed by considering a distribution of Stokeslets located along and directed parallel to the tail axis. The strengths of these Stokeslets must be such that the no-slip condition is satisfied on the surface of the combination body. This is not possible on the spherical portion of the body unless additional image singularities are introduced. Collins (1954) presented a method for determining a perturbed axisymmetric flow due to placing a sphere in a general unbounded Stokes flow field. Using this method, we can determine the flow field due to a single Stokeslet on the rod axis, thence by integration the effect of the entire rod.

Introduce a cylindrical co-ordinate system (r, ϕ, z) fixed in the body, with the positive-z axis directed along the after-body axis, cf. figure 1. Consider a Stokeslet of unit strength located on the tail axis at $z = z_*$ and directed in the negative-z direction. The stream function for the flow field due to this singularity is determined and decomposed, cf. appendix A, as

$$\psi(r,z) = \frac{r^2}{8\pi\mu[r^2+(z-z_*)^2]^{\frac{1}{2}}} - \frac{ar^2(3z_*^2-a^2)}{16\pi\mu z_*^2[r^2z_*^2+(zz_*-a^2)^2]^{\frac{1}{2}}} - \frac{a^3r^2(z_*^2-a^2)(zz_*-a^2)}{8\pi\mu z_*^2[r^2z_*^2+(zz_*-a^2)^2]^{\frac{3}{2}}} + \frac{a^3r^2(z_*^2-a^2)^2}{16\pi\mu z_*^2[r^2z_*^2+(zz_*-a^2)^2]^{\frac{3}{2}}}. \quad (1)$$

The first term in (1) is the original unit Stokeslet. The remaining three terms, which constitute the image system for this single Stokeslet, are, respectively, (i) a Stokeslet at the inverse point $z = a^2/z_*$, $r = 0$, with strength $a(3z_*^2-a^2)/2z_*^2$,

directed in the positive-z direction, (ii) a Stokes doublet (stresslet only) at the inverse point, with strength $a^3(z_*^2-a^2)/z_*^4$, directed in the z direction, and (iii) a source doublet at the inverse point, with strength $a^3(z_*^2-a^2)^2/2z_*^5$, directed in the z direction.

As a consistency check on (1), we can consider the limit $z_*-a\to 0$, in which case the flow between the Stokeslet and sphere resembles that outside a plane boundary. Taking $Z=z-a$ and $h=z_*-a$, we obtain

$$\psi \sim \frac{r^2}{8\pi\mu[r^2+(Z-h)^2]^{\frac{1}{2}}}-\frac{r^2}{8\pi\mu[r^2+(Z+h)^2]^{\frac{1}{2}}} -\frac{2hr^2(Z+h)}{8\pi\mu[r^2+(Z+h)^2]^{\frac{3}{2}}}+\frac{2h^2r^2}{8\pi\mu[r^2+(Z+h)^2]^{\frac{3}{2}}} \tag{2}$$

as $h\to 0$. Equation (2) agrees with the decomposition of the image system for a Stokeslet outside a no-slip plane wall, cf. Blake (1971).

The velocity field in the fluid is obtained from (1) as

$$\begin{aligned} v_r &= r^{-1}\partial\psi/\partial z \\ &= -\frac{r(z-z_*)}{8\pi\mu[r^2+(z-z_*)^2]^{\frac{3}{2}}}+\frac{a^3r(z-z_*)}{8\pi\mu[r^2z_*^2+(zz_*-a^2)^2]^{\frac{3}{2}}} \\ &\qquad +\frac{3arz_*(z_*^2-a^2)\,(zz_*-a^2)\,(r^2+z^2-a^2)}{16\pi\mu[r^2z_*^2+(zz_*-a^2)^2]^{\frac{5}{2}}} \\ &\equiv (8\pi\mu)^{-1}G(r,z;z_*), \end{aligned} \tag{3}$$

$$\begin{aligned} v_z &= -r^{-1}\partial\psi/\partial r \\ &= -\frac{2}{8\pi\mu[r^2+(z-z_*)^2]^{\frac{1}{2}}}+\frac{r^2}{8\pi\mu[r^2+(z-z_*)^2]^{\frac{3}{2}}}+\frac{2a}{8\pi\mu[r^2z_*^2+(zz_*-a^2)^2]^{\frac{1}{2}}} \\ &\qquad -\frac{a^3r^2-a(z_*^2-a^2)\,(r^2+z^2-a^2)}{8\pi\mu[r^2z_*^2+(zz_*-a^2)^2]^{\frac{3}{2}}}-\frac{3az_*^2r^2(z_*^2-a^2)\,(r^2+z^2-a^2)}{16\pi\mu[r^2z_*^2+(zz_*-a^2)^2]^{\frac{5}{2}}} \\ &\equiv (8\pi\mu)^{-1}H(r,z;z_*), \end{aligned} \tag{4}$$

where v_r and v_z are the radial and axial components of velocity, respectively.

3. Slender-body analysis

We now regard the tail of the body as a continuous distribution of Stokeslets of strength per unit length $F(z_*)$, $a<z_*<a+2l$, located on the axis $r=0$, and directed in the negative-z direction. The effects of this distribution, and of the uniform stream, are obtained by superposition:

$$v_r = U\left[-\frac{3arz}{4(z^2+r^2)^{\frac{3}{2}}}+\frac{3a^3rz}{4(z^2+r^2)^{\frac{5}{2}}}\right]+\frac{1}{8\pi\mu}\int_a^{a+2l}F(z_*)\,G(r,z;z_*)\,dz_*, \tag{5}$$

$$v_z = U\left[1-\frac{3a}{4(z^2+r^2)^{\frac{1}{2}}}-\frac{3az^2+a^3}{4(z^2+r^2)^{\frac{3}{2}}}+\frac{3a^3z^2}{4(z^2+r^2)^{\frac{5}{2}}}\right]+\frac{1}{8\pi\mu}\int_a^{a+2l}F(z_*)\,H(r,z;z_*)\,dz_*. \tag{6}$$

The no-slip condition on the tail surface is

$$v_z=0 \quad \text{at} \quad r=R(z), \quad a<z<a+2l. \tag{7}$$

Substituting in (6), we obtain the following integral equation for $F(z)$:

$$U\left[1-\frac{3a}{4(z^2+R^2)^{\frac{1}{2}}}-\frac{3az^2+a^3}{4(z^2+R^2)^{\frac{3}{2}}}+\frac{3a^3z^2}{4(z^2+R^2)^{\frac{5}{2}}}\right]+\frac{1}{8\pi\mu}\int_a^{a+2l}F(z_*)\,H(R,z;z_*)\,dz_*=0. \tag{8}$$

Since $R/2l \ll 1$ and $R/a \ll 1$, we have

$$\begin{aligned}U\left[\left(1-\frac{3a}{z}+\frac{a^3}{2z^3}\right)+O\left(\frac{R}{a}\right)^2\right]&\\+\frac{F(z)}{8\pi\mu}\left\{4\ln\left(\frac{2l}{R}\right)+2\ln\left[1-\frac{(z-a-l)^2}{l^2}\right]-2+I(z)+O\left(\frac{R}{l}\right)^2\right\}&\\+\lim_{R/l\to 0}\left[\frac{1}{8\pi\mu}\int_a^{a+2l}\{F(z_*)-F(z)\}\,H(R,z;z_*)\,dz_*\right]=0,&\end{aligned} \tag{9}$$

where the limit in the final term must be valid to $O(R/l)$. In the second term of (9), $I(z)$ represents the contribution of the image system:

$$I(z)=\frac{a(a^2-3z^2)}{z^3}\ln\left[\frac{z(a+2l)-a^2}{a(z-a)}\right]-\frac{4a^2l(z+a)}{z^2[z(a+2l)-a^2]}+\frac{2al(z+a)^2[z(a+l)-a^2]}{z^2[z(a+2l)-a^2]^2}. \tag{10}$$

We now expand $F(z)$ just as in classical slender-body theory, viz.

$$F(z)=\epsilon F^{(1)}(z)+\epsilon^2F^{(2)}(z)+\ldots\epsilon^nF^{(n)}(z)+\ldots, \tag{11}$$

where $\epsilon \equiv [\ln(2l/R_0)]^{-1}$, R_0 being a representative value of $R(z)$, for example the mean. This expansion, to order n, is applicable to (9) provided that

$$\epsilon^n = o[(R/l)^2, (R/a)^2].$$

We are in general interested in $l \geqslant a$. Thus, since $\ln(2l/R)$ increases much more slowly than $(l/R)^2$, the expansion could be carried to several orders. We shall, however, be interested in results to second order, since they embody the essential physics of the problem; i.e. they enable us to apply the no-slip condition to both the tail (first and second order) and head (second order) of the body. We obtain

$$F^{(1)}=2\pi\mu U(1-3a/2z+a^3/2z^3), \tag{12}$$

$$\begin{aligned}F^{(2)}=-\frac{\pi\mu U}{2}\left(1-\frac{3a}{2z}+\frac{a^3}{2z^3}\right)\left\{2\ln\left[1-\frac{(z-a-l)^2}{l^2}\right]-2+4\ln\left(\frac{R_0}{R}\right)+I(z)\right\}&\\+\frac{\pi\mu U}{2}\int_a^{a+2l}\left(\frac{3a}{2z}-\frac{3a}{2z_*}-\frac{a^3}{2z^3}+\frac{a^3}{2z_*^3}\right)H^{(1)}(z,z_*)\,dz_*,&\end{aligned} \tag{13}$$

where

$$\begin{aligned}H^{(1)}(z,z_*)&=\lim_{R_0/l\to 0}H(R,z;z_*)\\&=-\frac{2}{|z-z_*|}+\frac{2a}{zz_*-a^2}+\frac{a(z^2-a^2)(z_*^2-a^2)}{(zz_*-a^2)^3}.\end{aligned} \tag{14}$$

It is noteworthy that, in classical slender-body theory for a rod, the equivalent of the final term in (9) does not contribute to $F(z)$ until $O(\epsilon^3)$. Here, however, this term contributes to $F^{(2)}(z)$, i.e. there is a second-order coupling of image and tail singularity strengths. The rather lengthy complete expression for $F^{(2)}(z)$ is given

in appendix B. Although $F^{(1)}(z)$ is a well-behaved function of z, $F^{(2)}(z)$ is logarithmically singular at $z = a + 2l$. In order to integrate $F^{(2)}(z)$ with respect to z, we therefore adopt the procedure of Tillet (1970); i.e. we terminate the Stokeslets at $z = z_T$, where $l^{-1}(a + 2l - z_T) = O(\epsilon^2)$. Indeed, the integral force parameters, cf. § 4, are insensitive to $O(\epsilon^2)$ variations in the precise location of z_T. Notably, $F^{(1)}(z) \to 0$ and $F^{(2)}(z) \to 0$ as $z \to a$, i.e. the image Stokeslets obviate any singular behaviour at the forward end of the tail.

4. Force parameters

The total drag $\mathscr{F}$ on the combination body is given by

$$\mathscr{F} = 6\pi\mu a U + \int_{a^3/(a+2l)}^{a} \left(\frac{3z}{2a} - \frac{z^3}{2a^3}\right)\left[-F\left(\frac{a^2}{z}\right)\right] dz + \int_a^{a+2l} F(z)\, dz. \tag{15}$$

The first term in (15) is the familiar Stokes drag on an isolated sphere in a uniform stream. The second term is the corresponding reduction in drag on the spherical head of the combination body due to the internal image Stokeslets. The final term is the drag on the tail due to the axial Stokeslet distribution; this term and the force $F(z)$, $a < z < a + 2l$, per unit length on the tail are dependent upon the image system via (8). Using (11)–(13), we can rewrite (15) as

$$\mathscr{F} = \mathscr{F}_s + \mathscr{F}_t,$$

$$\begin{aligned}\frac{\mathscr{F}_s}{\pi\mu a U} = 6 + \epsilon\Bigg[&\frac{31}{140} + \frac{1-2\alpha(\alpha+1)}{(1+2\alpha)^2} - \frac{3}{2(1+2\alpha)^3} - \frac{1}{4(1+2\alpha)^4} \\ &+ \frac{3}{5(1+2\alpha)^5} - \frac{1}{14(1+2\alpha)^7}\Bigg] \\ + \epsilon^2\Bigg\{&\int_1^{1+2\alpha}\left(\frac{3}{2\eta^3} - \frac{1}{2\eta^5}\right)\left(1 - \frac{3}{2\eta} + \frac{1}{2\eta^3}\right)\Bigg[2 - 2\ln\left\{1 - \left(\frac{\eta-1-\alpha}{\alpha}\right)^2\right\} \\ &+ 4\ln\frac{R}{R_0} - I(a\eta)\Bigg] d\eta \\ &+ \frac{1}{4}\int_1^{1+2\alpha}\int_1^{1+2\alpha}\left(\frac{3}{\eta_*} - \frac{1}{\eta_*^2} - \frac{3}{\eta} + \frac{1}{\eta^3}\right)\left(\frac{1}{\eta^5} - \frac{3}{\eta^3}\right)\left(\frac{1}{a}\right) H^{(1)}(a\eta, a\eta_*)\, d\eta_*\, d\eta\Bigg\},\end{aligned} \tag{16a}$$

$$\begin{aligned}\frac{\mathscr{F}_t}{\pi\mu a U} = \epsilon&\left[4\alpha - 3\ln(1+2\alpha) + \frac{2\alpha(\alpha+1)}{(1+2\alpha)^2}\right] \\ &+ \epsilon^2\int_1^{1+2\alpha}\left(1 - \frac{3}{2\eta} + \frac{1}{2\eta^3}\right)\left\{1 - \ln\left[1 - \left(\frac{\eta-1-\alpha}{\alpha}\right)^2\right] + 2\ln\frac{R_0}{R} - \tfrac{1}{2}I(a\eta)\right\} d\eta,\end{aligned} \tag{16b}$$

where $\alpha \equiv l/a$, the subscripts s and t stand for 'sphere' and 'tail', respectively, and the expressions are correct to $O(\epsilon^2)$. Note that the shape of the tail, viz. $R(z)$, only influences the drag to $O(\epsilon^2)$, as is the case for an isolated slender body. The effect of the image system on $\mathscr{F}_t$ is $O(\epsilon^2)$, just as for a slender body near a plane wall, cf. de Mestre (1973). However, the images do produce an integrated effect $O(\epsilon)$ on $\mathscr{F}_s$.

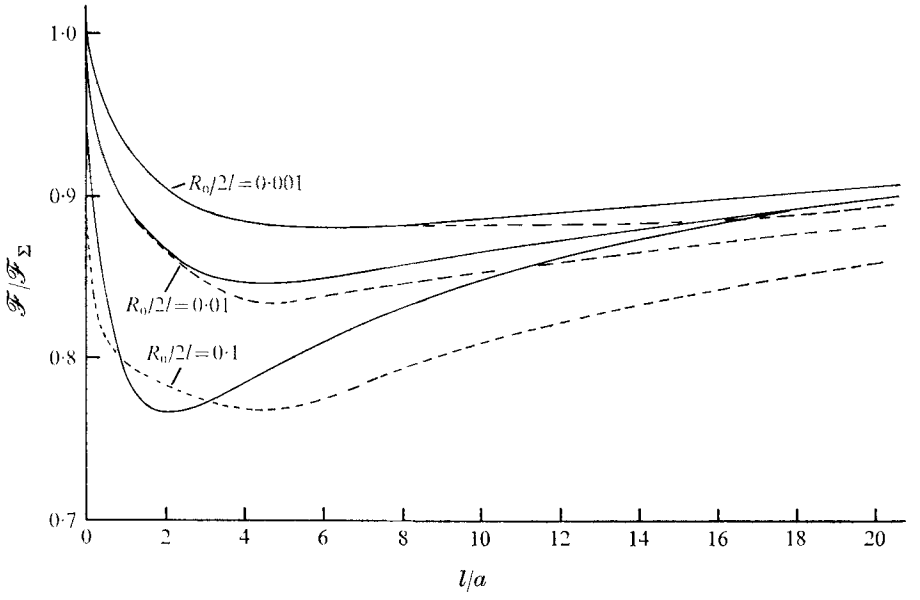

FIGURE 2. Comparison of the drag $\mathscr{F}$ with $\mathscr{F}_\Sigma$, the sum of the drags on the sub-bodies considered individually. ——, including image system; – – –, excluding image system.

5. Results and discussion

We now present and discuss several pertinent computations. For the sake of clarity here, we shall consider a constant tail radius R_0.

(i) The total drag $\mathscr{F}$ on the combination body may be compared with $\mathscr{F}_\Sigma$, the sum of the drags on an isolated sphere and on an isolated rod. The latter is simply

$$\mathscr{F}_\Sigma = 6\pi\mu aU + 4\pi\mu lU(\epsilon + 0{\cdot}807\epsilon^2), \tag{17}$$

correct to $O(\epsilon^2)$. The second term in (17) is obtainable from the method of analysis here, just as in Batchelor (1970), an identical expression being obtained from Cox (1970). The effect of combining the two bodies is to retard the after and forward flows experienced by the sphere and rod, respectively. Thus we generally expect $\mathscr{F} \leqslant \mathscr{F}_\Sigma$, with equality in the limits $l/a \to 0, \infty$. Curves of $\mathscr{F}/\mathscr{F}_\Sigma$ *vs.* l/a must therefore possess minima, as indicated by the mathematical form of $F^{(1)}(z)$, cf. (12). Figure 2 illustrates this result. Note that for truly slender bodies, i.e. $R_0/2l \lesssim 0{\cdot}01$, the drag on the combination body is reduced at most by $O(10\,\%)$ from that on the isolated bodies. Note also that, if the image singularities are neglected altogether, the error in $\mathscr{F}/\mathscr{F}_\Sigma$ is not substantial, decreasing with $R_0/2l$. For a typical mammalian spermatozoon, we might expect $l/a = 10$ and $R_0/2l = 0{\cdot}005$, where the effective radius a is that of a sphere with surface area equal to that of the sperm head and R_0 is an average tail radius. For these values, the error in $\mathscr{F}/\mathscr{F}_\Sigma$ is only $1{\cdot}2\,\%$. This suggests that in an analysis of flow about a more realistically shaped spermatozoon, for which the head is not spherical and $R(z)$ is not constant, a first approximation might be to neglect the image

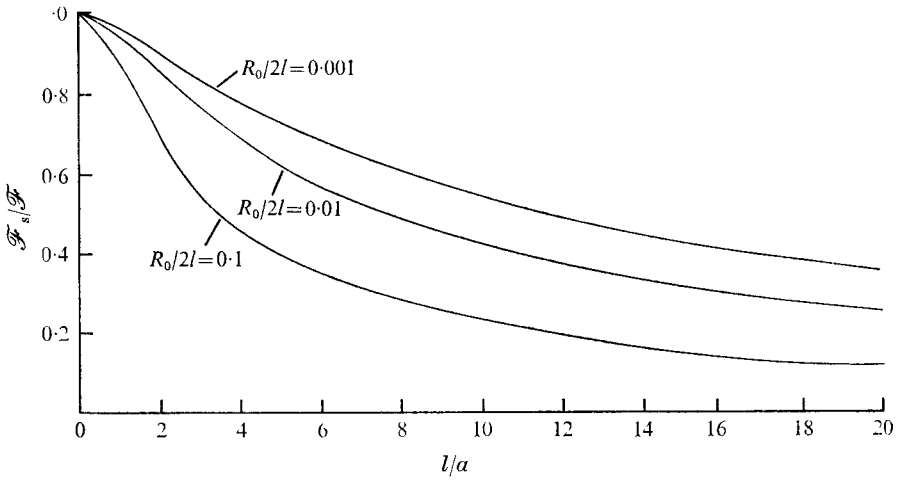

FIGURE 3. Comparison of the drag on the spherical head of the combination body with the total drag.

system altogether. Since extension of the Collins method to non-axisymmetric heads is extremely difficult at best, this would represent a very significant simplification. We are at present engaged in such an analysis.

(ii) The relative importance of the drags on the head and tail of the combination body may be assessed by considering the ratio $\mathscr{F}_s/\mathscr{F}$, cf. figure 3. Note the substantial reduction in the importance of the head drag for $l/a \geqslant O(10)$. For the sperm-like values $l/a = 10$ and $R_0/2l = 0{\cdot}005$, the head contributes 46% of the drag. Thus, quantitative interpretation of sedimentation experiments may be significantly in error if the effect of the tail is excluded, cf. Katz & de Mestre (1974).

(iii) In existing resistive-force (or Gray–Hancock) analyses of spermatozoan locomotion, the effect of the head has been accounted for only approximately. The viscous drag and moment included have been those on an isolated head, translating and rotating with the propulsive velocities, linear and angular, of the organism. The resistive effects of the actual, attached head are therefore overestimated. In figure 4 we have plotted the ratio $\mathscr{F}_s/6\pi\mu aU$. This ratio may be viewed as an upper bound (because the tail is straight) to the reduction in drag on the head of a motile swimming organism. Figure 4 indicates that the upper bound to this reduction does not differ appreciably from the case of an isolated head, as might be expected since the reduction is $O(\epsilon)$, cf. (16).

(iv) The resistive-force approach to spermatozoan locomotion has thus far neglected the influence of the head on the local resistances per unit length acting on an undulating tail. Indeed, account has not yet been taken of the influence of the finite length of the tail on these resistances. It is, therefore, of some interest to consider the local longitudinal force per unit length, i.e. Stokeslet strength, acting on the tail of our combination body. There exists a shielded region immediately behind the head in which this strength is significantly reduced from that on an isolated tail. The extent of this region suggests how im-

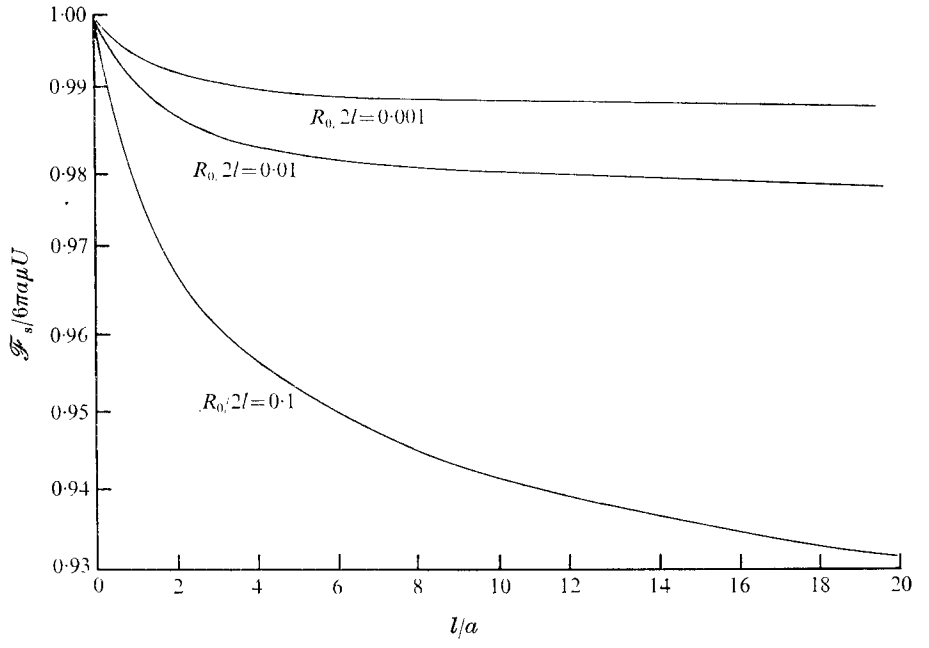

FIGURE 4. Comparison of the drag on the spherical head of the combination body with the drag on an identical, isolated sphere.

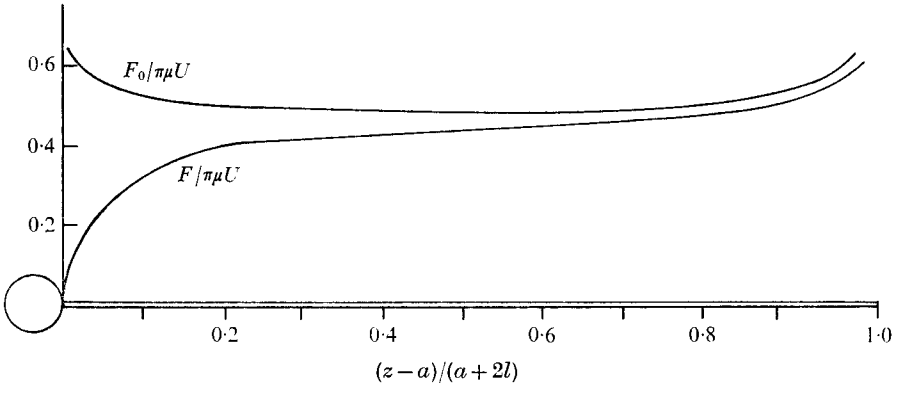

FIGURE 5. Comparison of the Stokeslet strength on the tail of the combination body with $F_0(z)$, the Stokeslet strength on an isolated tail; $l/a = 10$, $R_0/2l = 0·01$.

portant the shielding effect might be for a motile tail on an organism cum head. We therefore compare $F(z)$, along the tail of the combination body, with $F_0(z)$, the Stokeslet strength on an isolated, longitudinally translating tail. The latter is also obtainable from the analysis here, as in Batchelor (1970), as

$$F_0(z) = 2\pi\mu U\left[\epsilon+\tfrac{1}{2}\epsilon^2\left\{1-\ln\left[1-\left(\frac{z-a-l}{l}\right)^2\right]\right\}\right] \tag{18}$$

correct to $O(\epsilon^2)$. Figure 5 illustrates these strengths for the sperm-like body, the Stokeslets having been terminated at the ends of the tail, as mentioned

earlier, to avoid singularities. Note that along the first fifth of the tail of the combination body, i.e. four head radii, the strength is reduced by an average of approximately 50% from that on an isolated tail. We might argue, therefore, that along approximately this portion of the tail of a motile organism, there may be a need to introduce varying coefficients of resistance. Of course, account would have to be taken of a counter-effect, the thickening of the tail at its forward end, viz. the midpiece. However, the precise nature of the variation, in both longitudinal and normal coefficients, is a problem whose answer really cannot be suggested from the analysis here.

D.F.K. is grateful for the support of a Population Council Postdoctral Fellowship.

Appendix A

Suppose that $\psi_0(\rho, \theta)$ is a stream function satisfying the axisymmetric Stokes flow equation $D^4\psi_0 = 0$, where

$$D^2 \equiv \frac{\partial^2}{\partial\rho^2} + \frac{\sin\theta}{\rho^2}\frac{\partial}{\partial\theta}\left(\frac{1}{\sin\theta}\frac{\partial}{\partial\theta}\right)$$

and (ρ, θ, Φ) are spherical polar co-ordinates. If ψ_0 is the stream function for some flow in an unbounded fluid, then it can be shown, cf. Collins (1954), that the perturbed stream function due to the presence of a sphere of radius a is given by

$$\psi(\rho,\theta) = \psi_0(\rho,\theta) + \frac{\rho(\rho^2-3a^2)}{2a^3}\psi_0\left(\frac{a^2}{\rho},\theta\right) + \frac{\rho^2(\rho^2-a^2)}{a^3}\frac{\partial}{\partial\rho}\left[\psi_0\left(\frac{a^2}{\rho},\theta\right)\right]. \quad \text{(A 1)}$$

This solution produces zero velocity on the sphere and satisfies $D^4\psi = 0$, holding for singular and non-singular functions ψ_0.

For a Stokeslet at $(z_*, 0, 0)$, with unit strength and directed in the inward radial direction,

$$\psi_0 = \rho^2\sin^2\theta/8\pi\mu[\rho^2\sin^2\theta + (\rho\cos\theta - z_*)^2]^{\frac{1}{2}}. \quad \text{(A 2)}$$

The solution for such a Stokeslet outside a sphere, with centre at the origin, is therefore

$$\psi = \frac{\rho^2\sin^2\theta}{8\pi\mu[\rho^2\sin^2\theta + (\rho\cos\theta - z_*)^2]^{\frac{1}{2}}} - \frac{a\rho^2\sin^2\theta}{8\pi\mu[z_*^2\rho^2\sin^2\theta + (z_*\rho\cos\theta - a^2)^2]^{\frac{1}{2}}} - \frac{a\rho^2\sin^2\theta(z_*^2-a^2)(\rho^2-a^2)}{16\pi\mu[z_*^2\rho^2\sin^2\theta + (z_*\rho\cos\theta - a^2)^2]^{\frac{3}{2}}}. \quad \text{(A 3)}$$

When (A 3) is expressed in cylindrical polar co-ordinates (r, ϕ, z) it becomes

$$\psi(r,z) = \frac{r^2}{8\pi\mu[r^2 + (z-z_*)^2]^{\frac{1}{2}}} - \frac{ar^2}{8\pi\mu[z_*^2 r^2 + (zz_* - a^2)^2]^{\frac{1}{2}}} - \frac{ar^2(z_*^2-a^2)(r^2+z^2-a^2)}{16\pi\mu[r^2z_*^2 + (zz_*-a^2)^2]^{\frac{3}{2}}}. \quad \text{(A 4)}$$

Equation (A 4) can be separated into the expressions for the four basic singularities given in (1).

Appendix B

The complete expression for $F^{(2)}(z)$, the second-order component of the Stokeslet strength $F(z)$, can be written as

$$\begin{aligned}\frac{2}{\pi\mu U}F^{(2)} = &-\left(1-\frac{3}{2\eta}+\frac{1}{2\eta^3}\right)\left\{2\ln\left[1-\left(\frac{\eta-1-\alpha}{\alpha}\right)^2\right]-2+4\ln\frac{R_0}{R}+I(a\eta)\right\}\\
&+\left(\frac{6}{\eta}-\frac{2}{\eta^3}\right)\ln\eta-\frac{1}{\eta}\left[3\ln(1+2\alpha)+\frac{1}{2(1+2\alpha)^2}+\frac{1}{2}\right]\\
&-\frac{1}{\eta^2}\left(\frac{1}{1+2\alpha}+1\right)+\frac{1}{\eta^3}[\ln(1+2\alpha)+3]\\
&+(\tfrac{3}{2}\eta^2-\tfrac{5}{2}\eta)\left(1-\frac{1}{1+2\alpha}\right)+(\tfrac{1}{4}\eta^2-\tfrac{3}{4})\left[1-\frac{1}{(1+2\alpha)^2}\right]\\
&+(5-6\eta^2+3\eta^4)\ln(1+2\alpha)\\
&+\left(\frac{1}{2\eta^6}-\frac{3}{\eta^4}+\frac{9}{2\eta^2}-5+6\eta^2-3\eta^4\right)\ln\left[\frac{\eta(1+2\alpha)-1}{\eta-1}\right]\\
&+\left(\frac{1}{\eta^6}-\frac{4}{\eta^4}+\frac{9}{2\eta^2}+\tfrac{1}{2}-\tfrac{7}{2}\eta^2+\tfrac{3}{2}\eta^4\right)\frac{2\eta\alpha}{(\eta-1)[\eta(1+2\alpha)-1]}\\
&+\left(\frac{1}{4\eta^6}-\frac{5}{4\eta^4}+\frac{5}{2\eta^2}-\tfrac{5}{2}+\tfrac{5}{4}\eta^2-\tfrac{1}{4}\eta^4\right)\left\{\frac{1}{(\eta-1)^2}-\frac{1}{[\eta(1+2\alpha)-1]^2}\right\}, \quad \text{(B 1)}\end{aligned}$$

where $\eta \equiv z/a$ and $\alpha = l/a$.

REFERENCES

Batchelor, G. K. 1970 Slender-body theory for particles of arbitrary cross-section in Stokes flow. *J. Fluid Mech.* **44**, 419–440.

Blake, J. R. 1971 A note on the image system for a Stokeslet in a no-slip boundary. *Proc. Camb. Phil. Soc.* **70**, 303–310.

Collins, W. D. 1954 A note on Stokes's stream-function for the slow steady motion of viscous fluid before plane and spherical boundaries. *Mathematika*, **1**, 125–130.

Cox, R. G. 1970 The motion of long slender bodies in a viscous fluid. Part 1. General theory. *J. Fluid Mech.* **44**, 791–810.

Katz, D. F. & Mestre, N. J. de 1974 On the analysis of spermatozoan sedimentation. In preparation.

Mestre, N. J. de 1973 Low-Reynolds-number fall of slender cylinders near boundaries. *J. Fluid Mech.* **58**, 641–656.

Tillet, J. P. K. 1970 Axial and transverse Stokes flow past slender bodies. *J. Fluid Mech.* **44**, 401.